INFLUENCE OF SPATIALLY VARIABLE PRECIPITATION ON PASSIVE MARGIN ESCARPMENT EVOLUTION

BY

JESSICA SHIRLEY COLBERG

THESIS

Submitted in partial fulfillment of the requirements
for the degree of Master of Science in Geology
in the Graduate College of the
University of Illinois at Urbana-Champaign, 2011

Urbana, Illinois

Advisor:

Assistant Professor Alison Anders

ABSTRACT

Passive margin escarpments are large-scale geomorphic features which persist over timescales of tens of millions of years. The maintenance of steep topography over these timescales challenges conventional understanding of fluvial erosion. Typical explanations for passive margin escarpments rely on lithospheric flexure and fluvial network geometry. I suggest a role for interactions between climate and landscape evolution motivated by the Western Ghats of India. The Western Ghats experience a wet, tropical climate with topographically-controlled spatially varying precipitation. Precipitation reaches a maximum in the escarpment foothills and decreases sharply with elevation. Using a numerical landscape evolution model, I simulate the effects of coupled climate and topography on an idealized escarpment, including the effects of lithospheric flexure, pre-existing fluvial network geometry, and variability in bedrock resistance. Spatially varying precipitation enhances the slope and lifespan of an escarpment in a similar manner to a resistant bedrock ridge parallel to the escarpment crest. Precipitation variability is a viable mechanism for maintaining a steep escarpment, indicating that the lifetime of such geomorphic features may be a strong function of climate and precipitation mechanisms.

Table of Contents

INTRODUCTION

Current research highlights the role of differential erosion in dictating the dynamic behavior of the lithosphere during uplift and through the isostatic response to unloading (Thomson et al., 2010; Anders et al., 2010). Climate can play a strong role in creating differential erosion through spatial variations in temperature and precipitation. By doing so, it acts as a control on topographic evolution, yet climate itself reacts strongly to topography. The presence of mountains can both enhance precipitation and create rain shadows (Smith, 1979; Roe, 2005). These feedbacks create a coupled system whereby topography and climate evolve concurrently (Beaumont et al., 1992; Roe et al., 2002; 2003; Anders et al., 2008). I suggest a mechanism by which the morphology of a passive margin escarpment and orographically controlled precipitation gradient reinforce each other over long timescales.

Passive margin escarpments offer an opportunity to investigate the effects of spatially varying precipitation on long-term landscape evolution in a tectonically quiescent setting. Passive margin escarpments occur in areas which have experienced continental rifting and typically have a steep, coast parallel morphology on the order of hundreds of kilometers long (Matmon et al., 2002). Despite the lack of active tectonic uplift, passive margin escarpments remain high and steep for tens of millions of years after rifting, raising important questions about their geomorphic evolution (Tucker and Slingerland, 1994; Gunnell and Fleitout, 1998;Matmon et al., 2002; Braun and van der Beek, 2004). Namely, how is the observed steep, high topography maintained in the absence of tectonic uplift?

Multiple models have been suggested for the erosional development of passive margin escarpments. Some researchers suggest that the escarpment evolves through long term parallel retreat or by plateau downwearing (Braun and van der Beek, 2004; Campanile et al., 2008).

Others argue that the landform remains stable after an initial period of intense erosion (Matmon et al., 2002). Tucker and Slingerland (1994) conclude that the escarpment forms at the time of rifting and evolves through parallel retreat. Van der Beek and Braun (1999) assert that the escarpment forms in place, eroding out of a downwearing plateau. Based on lack of evidence for continued, long term retreat, Matmon et al. (2002) envision a less dynamic landform with a period of intense erosion and retreat shortly after rifting following by long periods of stability. Campanile et al. (2008) endorse a parallel retreat model for the Western Ghats of India.

Researchers agree that the location of the drainage divide is important in determining escarpment evolution (Tucker and Slingerland, 1994; Matmon et al., 2002; Braun and van der Beek, 2004). When the drainage divide is located at the escarpment crest, the headwaters of rivers draining the escarpment have limited drainage areas and proportionally small discharges. In order to transport sediment and erode into bedrock, these reaches must be very steep, favoring an escarpment morphology (van der Beek and Braun, 1999). The effect is reinforced because streams on the interior plateau of the escarpment drain away from the rift, preventing streams on the steep slope of the escarpment from capturing large drainage areas through stream piracy (Tucker and Slingerland, 1994).

Factors suggested as major controls on escarpment evolution include the thermal influence of rifting (Campanile et al., 2008), lithospheric flexure (Gunnell and Fleitout, 1998, Campanile et al., 2008), pre-existing fluvial network geometry (Tucker and Slingerland, 1994), and variability in rock hardness (Gunnell and Harbor, 2008). During and after rifting, high temperatures make the rifted crust isostatically buoyant, leading to uplift at the edge of the plate for timescales on the order of a few tens of millions of years (Gunnell, 2001a). However, lithospheric flexure in response to erosional unloading may cause a similar, longer-lived effect

(Campanile et al., 2008). Flexural uplift increases the lifespan of high elevation topography as the deep crustal root isostatically rebounds after denudation (Turcotte and Schubert, 2002). Additionally, flexural uplift may help to pin drainage divides near the crest of the escarpment (Gunnell and Fleitout, 1998; Campanile et al., 2008). Because the flexural wavelength of the lithosphere is greater than the width of the escarpment, uplift in response to denudation of the coastal plain raises the escarpment as well, tilting the escarpment away from the rift and limiting the headward migration of the divide (Tucker and Slingerland, 1994). Lithology plays a role in escarpment evolution as well, and in cases with extremely slow rates of retreat, resistant lithologies may play an important role in pinning the location of the escarpment (Matmon et al., 2002; Harbor and Gunnell, 2007). All of these suggested controls on escarpment evolution help to maintain the drainage divide at or near the escarpment crest.

Motivated by the Western Ghats of India, I investigate another possible control on escarpment evolution: topographically-controlled spatial variability in precipitation. The Ghats experience intense seasonal precipitation strongly controlled by topography (Figure 1). Orographic effects create a strong spatial variation in precipitation with large precipitation totals falling on the coastal plain intensifying to a maximum near the toe of the escarpment and sharply decreasing to comparatively low precipitation rates on the interior plateau (Madhavan, 2009). Paleoclimatic proxies suggest that the monsoon has been occurring for at least 8-22 Ma (Dettman et al., 2001; Clift et al., 2005). As such, the Western Ghats have experienced a strong, topographically-controlled precipitation gradient over time scales relevant to long term escarpment evolution, the effects of which are worthy of investigation.

The Western Ghats run parallel to the coast of India for approximately 1600 km. Morphologically, they are made up of a coastal plain roughly 30 km wide, a coast-parallel

escarpment with average height of 900 m, and an interior plateau that dips gently towards the eastern coast (Figure 2). Along most of their length, the continental drainage divide roughly coincides with the crest of the escarpment. The Ghats vary lithologically from the basaltic Deccan Traps in the north to high-grade Precambrian metamorphic rocks of the Dharwar Craton in the south (Harbor and Gunnell, 2007).

In the Dharwar Craton section, scarp-parallel Archean folds and metamorphic fabric affect scarp retreat and drainage network geometry (Gunnell, 2001b; Harbor and Gunnell, 2007). Just beyond the southern limit of the Deccan Traps is a region known as the Ghats Breaches in which the drainage divide is not closely associated with the top of the great escarpment. Several rivers have captured significant drainage areas on the interior plateau (Harbor and Gunnell, 2007). The scarp parallel orientation of the river networks has allowed large scale drainage piracy by streams draining the escarpment face. When the headward erosion of a west-draining river breaches the large, low gradient, scarp-parallel basin of a river on the interior plateau, the west-draining stream can redirect flow in the entire basin towards the west. Farther south, linear sections of the escarpment represent local resistant structural features in highly resistant granulite terrain (Harbor and Gunnell, 2007).

The lithosphere in the Western Ghats region has a low elastic thickness. In the absence of active tectonics, lithospheric flexure is an important cause of ongoing uplift. Gunnell and Fleitout (1998) modeled the Ghats lithosphere as a 'broken' plate with minimal coupling between a 1.3 km thin elastic plate offshore and a thick plate onshore with elastic thickness of 70 km. Campanile et al. (2008) concluded that a continuous plate with elastic thickness of 10 km produced an amount of rock uplift near the escarpment consistent with a model of an uplifted rift scarp undergoing denudation and parallel retreat. Elastic thicknesses up to 30 km, while

producing smaller magnitudes of uplift, still caused maximum uplift close to the escarpment. These studies agree that the Western Ghats is an area of flexurally weak lithosphere, indicating that the region can experience a significant, local flexural response due denudational unloading.

The purpose of this study is to evaluate the ability of topographically-controlled spatially-varying precipitation to maintain or even enhance steep topography over long timescales. The Western Ghats offer a real world example of a topographically-controlled precipitation gradient over a long-lived regional scale escarpment. Using factors observed in the Western Ghats, I model the evolution of an idealized passive margin escarpment under the influence of differences in precipitation pattern, bedrock resistance, and flexural parameters.

METHODS

The goal of the project is not to model the topographic evolution of the Western Ghats or to predict the future of the escarpment, but to evaluate the qualitative effect of topographically-controlled spatial variations in precipitation on the evolution of a passive margin type escarpment. To test the effects of spatially varying precipitation on escarpment evolution, I use the numerical surface processes model CASCADE (Braun and Sambridge, 1997) with a simple precipitation function coupled to topography. CASCADE routes precipitation across the landscape with a bucket-passing algorithm. A stream power relation determines the erosion at each node during each time step, calculated by:

$$E = kSQ^{0.5} \qquad (1)$$

where Q is the discharge reaching the node from upstream drainage area, S is slope at the node, and *k* is a constant that varies with lithology (Stock and Montgomery, 1999). Eroded material is assumed to leave the domain during each time step. The model includes threshold-slope landsliding for short-range transport (Anders, 2005).

In the case of a tectonically inactive passive margin escarpment undergoing large scale denudation on geologic time scales, lithospheric flexure is a source of ongoing uplift and can play a role in pinning the drainage divide (Tucker and Slingerland, 1994). CASCADE uses a spectral method to solve the fourth order differential equation for the deflection of an elastic plate:

$$D\frac{d^4w}{dx^4} = q(x) - P\frac{d^2w}{dx^2} \qquad (2)$$

(Turcotte and Schubert, 2002). Modeling and offshore sedimentary records suggest that the plate beneath the Western Ghats has a low flexural rigidity, best modeled by a broken plate with weak lithosphere at the edge of the passive margin and greater flexural thickness inland (Campanile et

al., 2008; Gunnell and Fleitout, 1998). Because CASCADE cannot model spatial differences in flexural thicknesses, I selected a reasonable flexural thickness (T_e) of 30 km based on models by Gunnell and Fleitout (1998) and tested the sensitivity of the model to changes in T_e.

The Western Ghats experience intense seasonal precipitation as part of the South Asian Summer Monsoon (Grossman and Durran, 1984). The presence of the escarpment affects regional climate by acting as a barrier to low level monsoon winds offshore (Grossman and Durran, 1984). The barrier plays a role in triggering deep convection, which is a significant factor in the monsoon precipitation experienced in the region (Grossman and Durran, 1984). The Tropical Rainfall Measurement Mission (TRMM) is a joint project between the NASA and the Japan Aerospace Exploration Agency to take satellite measurements of tropical and subtropical precipitation. The measurement accuracy is sufficient to resolve spatial precipitation gradients in areas with large daily precipitation values such as the Western Ghats (Nesbitt and Anders, 2009). TRMM precipitation measurements in the Western Ghats can be correlated with elevation, showing a maximum at low elevations and decreasing precipitation at higher elevations (Figure 1).

To investigate the coupled relationship between topography and precipitation, the model must include a rain function that is dynamically related to topography. Elevation can serve as a simple proxy to simulate the complex convective atmospheric processes which produce the observed rain pattern. By relating precipitation to elevation, I create a dynamic rain function that models the evolving responses between topography and climate over long timescales. To do so, a Gaussian distribution centered at the elevation of the foothills disperses a limited amount of water vapor across the landscape from west to east (Equation 3). I adjust the center, width, and height of the bell curve to match the observed relationship between precipitation and elevation in

the Ghats (Figure 1). Evaluated recursively from west to east, the equation for precipitation at each node is

$$P = C_3\left(C_1 + C_2 G(i)\right)\frac{w}{w_{tot}} \quad (3)$$

where C_3, C_2, and C_1 are constants, $\frac{w}{w_{tot}}$ is the fractional water remaining, and $G(i)$ is a gaussian distribution of the form

$$G(i) = G_{max} e^{\frac{-(h(i)-G_{center})^2}{2G_{width}^2}} \quad (4)$$

where i is the node index and $h(i)$ is the elevation at that node (Figure 3).

To determine the importance of spatially varying precipitation to escarpment evolution, I compare simulations of idealized escarpments experiencing different rain patterns and different patterns of bedrock resistance (Table 1). The uniform rain function equally distributes a volume of water over the landscape that is equal to the volume of water distributed by the dynamic rain function over the initial topography, a value of 0.7935 m/yr for the initial conditions described below. This average value does not change significantly when integrated over all time steps in a control model run, indicating that the average over the initial time step is an effective proxy for the average of the total volume of water over the entire simulation of the dynamic rain function.

To simulate the effects of variable resistance in bedrock structures and lithology, I placed a north-south running bedrock ridge with doubled bedrock resistance from x=40-50 km into an idealized escarpment experiencing the uniform rain function previously mentioned. The model distinguishes the bedrock resistance by changes in the fluvial erosion constant, *k*, in the model's stream power erosion law (Equation 1). Reasonable values for *k* of metamorphic rocks were chosen in accordance with the metamorphic lithology of the Dharwar craton (Stock and Montgomery, 1999). Increases in kduring the variable bedrock resistance simulation were

contained within this range of reasonable values (Stock and Montgomery, 1999). Simulations tested the effects of a bedrock ridge with two times greater resistance and one with ten times greater resistance.

The initial topography used in the model runs represents an idealized passive margin escarpment (Figure 3). The initial conditionsinclude a 1000 m high escarpment located at 30 km from the western side of a 400 km wide domain. Slopes are initially gentle, rising linearly from either coast to the escarpment crest. The initial escarpment crest represents a pre-existing drainage divide, in accordance with the recognized important of a drainage divide located at or near the escarpment crest. The parameters of the idealized escarpment represent reasonable values for a passive margin escarpment, using the Western Ghats as a guide. The height of 1000 m is reasonable for the Ghats, as is the distance from the coast to the escarpment crest of 30 km. The width of the domain is 400 km, a reasonable width for the Indian subcontinent in the southern region. The nature of the initial topography puts the drainage divide at the top of the escarpment, matching the drainage divide location for most of the Western Ghats. Topography varies only in one direction, which is a good first order approximation to the morphology of the Western Ghats escarpment.

RESULTS

Escarpment lifespan

To compare the results of the different simulations, it is useful to quantify the endurance of high topography as the escarpment evolves. For the purposes of this study, lifespan is defined to mean the time the escarpment takes to erode to 50% of its initial maximum height. Reasonable values for the constant of fluvial erosion (Stock and Montgomery, 1999) create simulated escarpments with lifespans on the order of tens of millions of years. This result is consistent with lifespans observed in real passive margin escarpments.

Spatially varying precipitation

The dynamic rain simulation produces an escarpment lifespan of 37 Ma (Table 2). Precipitation intensity is focused at the toe of the escarpment while the higher elevations and the plateau receive comparatively little rain. Under these conditions, the initial topography undergoes an immediate steepening along the escarpment face (Figure 4a). The increase in slope is most significant at the toe of the escarpment. The escarpment maintains the profile shape achieved by this initial steepening throughout the lifespan of the escarpment, even as it decreases in elevation (Figure 4b,c). A graph of the slope at the midpoint of the escarpment through time confirms this result. The slope increases steadily for the first 15 Ma of the run, then oscillates around a constant value before fading away as the escarpment erodes entirely away. Topographically-controlled spatially varying precipitation produces a long-lived, steep escarpment with a precipitation-topography relationship similar to that observed in the Western Ghats.

Comparison of dynamic and uniform rain functions

Similar to the dynamic rain simulation, uniformly distributed rain results in an immediate steepening of the escarpment due to the relationship between drainage area and erosion rate. Rivers are more erosive at the toe than they are near the drainage divide at the crest of the escarpment. However, the immediate steepening produced by the uniform rain function is not as extreme as that produced by the dynamic rain function. A comparison of the cross-sections of dynamic and uniform rain simulations reveals that the profile of the escarpment experiencing uniform rain has gentler slopes than the profile of the escarpment experiencing dynamic rain (Figure 4). The midpoint slope confirms the difference in profile; the uniform rain simulation produces consistently shorter slopes for the entirety of the escarpment's lifespan (Figure 6).

The escarpment erodes more quickly under a uniform rain pattern than it does in the dynamic rain simulation, making it difficult to directly compare escarpment morphology over time between dynamic and uniform rain. Compared to a lifespan of 37 Ma for dynamic rain, the uniform rain simulation produces a lifespan of 25 Ma (Table 2). In the uniform rain simulation, the intense precipitation which was focused on the foothills is spread evenly over the model domain. Effectively, the diminished lifespan indicates that precipitation is more efficient in eroding the landscape when it is evenly distributed.

To compare the profiles at similar stages of escarpment evolution, cross-sections were plotted at percentages of the initial maximum height (Figure 5). When the cross-sections are compared at similar heights, the profile shape of the uniform rain simulation is significantly gentler in slope than the dynamic rain simulation, especially at the toe of the escarpment. The difference in profile shape is consistent with the graph of slope vs. time, in which the slope of the uniform rain simulation is always lower than that of the dynamic rain simulation. These

comparisons confirm that the different rain functions produce real differences in escarpment morphology as well as lifespan.

Spatially varying bedrock resistance

The lifespan of the escarpment under uniform rain increases with the addition of a resistant bedrock ridge parallel to the escarpment. Without specific measurements of bedrock resistance in a region, the magnitude of variation in k is qualitative rather than quantitative. For example, a ridge with two times greater resistance increases the escarpment lifespan under uniform rain from 25 Ma to 35 Ma, a lifespan on the order of the escarpment under a dynamic rain pattern. Increasing the resistance by ten times increases the lifespan to more than 100 Ma, greater than the length of the simulation. The latter produces a bizarre, monolithic ridge surrounded on either side by a flat plain.

When a bedrock ridge with twice the resistance of the surrounding area is present, the simulated lifespan of the escarpment is similar to that observed in the dynamic rain simulation. This similarity allows me to compare and contrast the effects of resistant bedrock structures to the effects of spatially varying precipitation on escarpment morphology. When cross sections are compared at similar times the face of the escarpment in the resistant bedrock simulation does not show the long-lived steepness observed in the dynamic rain case through its lifespan (Figure 4). When compared at similar heights, the resistant ridge shows greater similarity to the profile of uniform rain than to dynamic rain (Figure 5). Only in Figure 5a does the bedrock resistance simulation appear to approach the steepness of the dynamic rain. This period of increased steepness is confirmed by the slopes in Figure 6. The temporary spike in the slope of the variable bedrock resistance run represents the moment that the crest of the eroding escarpment

reached the resistant bedrock ridge located at x=40 km (Figure 6). However, once the escarpment crest has eroded into the ridge, the slopes begin to shallow.

Hypsometry

Differences in morphology can also be seen using hypsometry. A hypsometric curve is the normalized frequency curve of area over elevation (Strahler, 1952). In a model domain with a grid of nodes, the hypsometric curve can be conceptualized as recording the fraction of nodes at each elevation. Figures 9 -12 show hypsometric curves for the steep side of the escarpment at 0 Ma, 5 Ma, 10 Ma, and 20 Ma for patterned rain, uniform rain, and bedrock ridges with two-times and ten-times greater resistance. These curves represent times in the simulation when the escarpment morphology has formed in all runs but before it has lost a significant portion of its height. Initially for all runs, area is distributed evenly over all elevations, a feature of the initial idealized escarpment morphology (Figure 3).

The hypsometric curve for patterned rain shows a bench in the area distribution at middle elevations. This drop reflects the effect of the precipitation pattern on the landscape. The dynamic rain function focuses precipitation at middle elevations on the foothills of the escarpment. These elevations experience the most intense erosion and show lower frequencies of occurrence. With less area at mid elevation, the landscape increases sharply from low to high elevations. In other words, this bend in the hypsometric curve represents the effect of the steep escarpment in the distribution of elevation over the landscape.

Hypsometric curves for uniform rain and for variable bedrock resistance do not show this distinct bend in the hypsometric curve at mid-elevations. Uniform rain and variable bedrock resistance runs have similar shapes in their hypsometric curves. Even with a bedrock ridge with

resistance increased by a factor of ten, the shape of the hypsometric curve looks very similar to the curve of the uniform rain simulation. The only difference is a notch at the highest elevations representing the increased endurance of the top of the resistant ridge. Based on the similar shapes in hypsometric curves, the presence of a resistant, scarp-parallel bedrock ridge in a simulation with uniform rain increases the escarpment lifespan but does not change the landscape shape dramatically. Morphologically, dynamic rain produces significantly different results contrasted with uniform rain and variable bedrock resistance.

Flexural Sensitivity Tests

Increasing the elastic thickness of the lithosphere produce escarpments with shorter lifespans (Table 2). By 37.5 Ma, the escarpment with an elastic thickness = 70 km has eroded almost entirely while the escarpment with an elastic thickness = 5 km is still at approximately 80% of its original height (Figure 7c). An elastic thickness of 5 km gives an escarpment lifespan of 44 Ma, 30 km a lifespan of 37 Ma, and 70 km a lifespan of 34 Ma. Slope of the escarpment does not change with increasing elastic thickness, indicating that elastic thickness affects escarpment lifespan but not morphology (Figure 8).

DISCUSSION

Model results indicate that escarpment lifespan and escarpment slope are independent characteristics which can be separately influenced by different controls such as elastic thickness of the lithosphere, precipitation pattern, and variability in bedrock resistance. Escarpment lifespan is affected by elastic thickness, variability of bedrock resistance, and rain pattern. Escarpment slope increases significantly over time as a result of spatially varying precipitation and spatially varying bedrock resistance. The effect of resistant bedrock structures on the slope of the escarpment changes depending on the relative position of the escarpment and the resistant bedrock structure and on their evolution through time. Spatially varying precipitation, however, emerges as the most important control examined in maintaining and enhancing a steep slope through the lifespan of the escarpment. The elastic thickness of the lithosphere influences the lifespan of the escarpment without significantly changing the slope of the escarpment. .All of the controls investigated in this study relate to the real world scenario of the Western Ghats Great Escarpment which is characterized by intense tropical rainfall, low elastic thicknesses, and resistant scarp-parallel bedrock lithology.

Elastic thickness exerts a direct control on the escarpment lifespan but does not play a role in enhancing escarpment slopes. The elastic thickness of the lithosphere dictates the effectiveness of local flexural response to erosional unloading. Lower elastic thicknesses reflect a more flexible lithosphere which can respond locally to the denudation of the coastal plain, causing sustained uplift of the escarpment crest proximal to the coastal plain. With a higher elastic thickness, the internal strength of the lithosphere is greater and the effects of denudation are spread over much larger areas, leading to a weaker local response. In this way, lower elastic thicknesses increase the lifespan of the escarpment. A lower elastic thickness does not change

the slope of the escarpment because the escarpment is uplifted as a unit (Figure 8). The wavelength of the flexural response, even a small elastic thickness is too large to cause differential uplift across the escarpment. The consistency in slope over different elastic thicknesses suggests that flexural response which helps to maintain a drainage divide concurrent with the scarp crest is not as important in controlling escarpment slope as patterned rain and variable bedrock resistance.

The presence of a resistant bedrock ridge increases the lifespan of the escarpment without significantly changing the escarpment shape except when the escarpment crest is located at the boundary of the bedrock structure. When a bedrock ridge ten times more resistant to erosion than surrounding regions is present, the escarpment has a lifespan of more than 100 Ma. The impressive increase in lifespan suggests that variations in bedrock resistance can easily dominate other controls on escarpment lifespan. However, the more interesting case for comparison is the bedrock ridge with two-times greater resistance, which has a lifespan comparable to that of the dynamic rain simulation. There is a 10 Ma difference in lifespan between the two-times greater bedrock resistance simulation and the uniform rain simulation, but morphologically the two runs are very similar. Comparing escarpment cross sections at the same stage of denudation shows similar shapes of the face of the escarpment (Figure 5). The hypsometric integrals are also very similar (Figures 10 and 11). The variable bedrock resistance run shows only a small increase in the abundance of the highest elevations, reflecting the slightly longer-lived high topography at the top of the resistance ridge (Figure 11).

The biggest difference in morphology between the uniform rain run and the two-times greater bedrock resistance run can be seen in the figure of mid-point slope vs. time (Figure 6). The moment that the retreating escarpment reaches the resistant bedrock ridge is visible in this

figure as a jump in the slope. At this time, the slope of the escarpment with the resistant bedrock ridge is briefly greater than the slope of the patterned rain run. At the margin of the bedrock structure, the difference in resistance between the escarpment crest and the coastal plane is at a maximum, leading temporarily to a situation with intense erosion focused at the toe of the escarpment, similar to the effects of the dynamic rain pattern. However, in the case of variable bedrock resistance, the effect fades as the escarpment crest continues retreating through the resistant ridge. As such, in a passive margin where scarp retreat is controlled by lithologic variation, the slope of the escarpment may depend on the position of the scarp relative to existing bedrock structures.

Spatially varying precipitation produces an increased lifespan of high topography and steeper slope relative to uniform precipitation simulations. By focusing the highest precipitation at the toe of the escarpment, the face of the escarpment continues to steepen while the relative weaker precipitation at higher elevations only minimally erodes the crest and interior plateau. The high volume of water focused on the toe of the escarpment has significant erosive power when spread evenly over the domain in the uniform rain run, leading to an escarpment lifespan with is 12 Ma less than the lifespan of the escarpment experiencing patterned rain. In addition to an increased lifespan, spatially varying precipitation has a sustained positive effect on escarpment slope through time (Figure 6). The magnitude of the effects of spatially varying precipitation on overall escarpment morphology are easily seen by comparing the hypsometric curves of patterned rain, uniform rain, and variable bedrock resistance (Figures 9-12). Compared to variable bedrock hardness and changes in elastic thickness, spatially varying precipitation has a distinct, lasting effect on escarpment slope over the lifespan of the escarpment. The impact of high volumes of water on the landscape is very relevant to the intense, tropical precipitation

experienced by the Western Ghats of India. Results suggest that the distribution of the precipitation on the landscape can play an important role in maintaining and enhancing escarpment lifespan and slope even in a climate where intense precipitation can create correspondingly high discharges in the fluvial networks that erode the escarpment.

Both spatially varying precipitation and variable bedrock resistance can have positive effects on escarpment lifespan and slope. In the case of variable bedrock resistance, the positive effects on slope are not continuous for the entire lifespan of the escarpment due to changes in the resistant ridge over time. It is difficult to compare these mechanisms directly because the magnitude of their effects on escarpment lifespan, height, and slope can be altered by adjusting input parameters. Both have positive effects on the lifespan of steep, high topography when compared to a model domain with homogenous bedrock resistance and a uniform rain pattern. Because the effects of variable bedrock resistance depend on the location, orientation, and erosional coefficient of the resistant lithologic structure, the effect of variable bedrock resistance changes as the resistant structure evolves through time. Spatially varying precipitation produces more consistent effects through time because the precipitation pattern has a self-sustaining aspect due to its dependence on elevation. In effect, the elevation-dependent precipitation pattern maintains the same escarpment morphology which produces it.

For a field location like the Western Ghats of India, identifying the dominant mechanism controlling escarpment evolution is complex. In the case of the modeled escarpment, the escarpment's position on the slope vs. time curve determines which factor is currently exerting the strongest control on escarpment morphology. In the case of the Western Ghats, it would be difficult to distinguish between the effects of regionally scarp-parallel resistant folds and fabrics and the monsoon precipitation gradient. Based on modeled results, basin hypsometry in the

Ghats may be a useful tool in distinguishing which factors are currently controlling escarpment evolution. It is likely that both these mechanisms play a role in the evolution of the Western Ghats escarpment. Additionally, the low elastic thickness at the continental margin (Campanile et al., 2008; Gunnell and Fleitout, 1998) augments the tendency of resistant structures and patterned rain to increase escarpment lifespan and slope by allowing greater local flexural compensation for denudation of the coastal plain. As such, spatial variations in lithology and spatially varying precipitation are competing, effective controls on the evolution of long-lived escarpments with high, steep topography such as the Western Ghats.

CONCLUSIONS

Numerical model simulations provide criteria by which to evaluate proposed controls on the evolution of long-lived high, steep topography of passive margin escarpments in the absence of tectonic forcing. Fluvial network geometry, variability in bedrock resistance, and lithospheric flexure have been previously suggested as controls on escarpment evolution and are included in the model runs. I suggest that topographically-controlled, spatial variability in precipitation is another significant control on escarpment evolution. In an idealized simulation, spatially varying precipitation coupled to topography maintains and enhances escarpment height and steepness over long time periods. Results also support the effectiveness of spatial variability in bedrock resistance as a control on escarpment lifespan and slope, dependent on the location of the resistant structure relative to the scarp crest.

Such spatial variability in precipitation is observed in the Western Ghats and has likely been a factor for tens of millions of years (Dettman et al., 2001; Clift et al., 2005). Determining the relative importance of factors like precipitation gradient and patterns of resistant lithology in the field is complex. Model results suggests the relative importance of these controls can change as the escarpment evolves. However, model results also suggest morphological differences that results from the dominance of different factors, which may be detectable in the field. The numerical models presented here indicate that spatial variability in precipitation is potentially significant control on passive margin evolution.

Future work will investigate the effects of topographically controlled precipitation on the valley scale and its potential effects on the regional sinuosity of the escarpment. Model simulations will make use of remotely-sensed real topography to evaluate the effects of a dynamic rain function on complex topography and the evolution of individual valleys.

REFERENCES

Anders, A. M.(2005), The Co-evolution of precipitation and topography, Ph.D. thesis, University of Washington, Seattle, WA.

Anders, A. M., G. H. Roe, D. R. Montgomery, and B. Hallet (2008), Influence of precipitation phase on the form of mountain ranges, *Geology*, 36, 479-82, doi: 10.1130/G24821A.1

Anders, A.M., S.G. Mitchell, and J.H. Tomkin (2010), Cirques, peaks, and precipitation patterns in the Swiss Alps: Connections among climate, glacial erosion, and topography, Geology, 38, 239-242, doi: 10.1130/G30691.1.

Beaumont, C., P. Fullsack, and J. Hamilton (1992), Erosional control of active compressional orogens, in *Thrust Tectonics*, edited by K. R. McClay, pp. 1-18, Chapman and Hall, New York.

Braun, Jean, and Malcolm Sambridge (1997), Modeling landscape evolution on geological time scales: a new method based on irregular spatial discretization, *Basin Research*, 9, 27-52, doi: 10.1046/j.1365-2117.1997.00030.x.

Braun, J., and P. van der Beek, (2004), Evolution of passive margin escarpments: What can we learn from low-temperature thermochronology, *Journal of Geophysical Research*, 27, F4009, doi: doi:10.1029/2004JF000147.

Campanile, D., C. G. Nambiar, P. Bishop, M. Widdowson, and R. Brown (2008), Sedimentation record in the Konkan-Kerala Basin: Implications for the evolution of the Western Ghats and the Western Indian passive margin, *Basin Research*, 20, 3-22, doi: doi:10.1029/2004JF000147.

Clift, P.D. et al. (2008), Correlation of Himalayan exhumation rates and Asian monsoon intensity. *Nature Geoscience*,1, 875-880, doi: 10.1038/ngeo351.

Dettman, D. L. et al. (1998), Seasonal stable isotope evidence for a strong Asian monsoon throughout the past 10.7 m.y., *Geology*, 29, 31-34, doi: 10.1130/0091-7613(2001) 029<0031:SSIEFA>2.0.CO;2

Grossman, R.L., and D.R. Durran (1984), Interaction of low level ow with the Western Ghat mountains and off-shore convection in the summer monsoon. Monthly Weather Review, 112, 652-672.

Gunnell, Y. (2001a), Morphology and Scarp Recession Rates of the Western Ghats Escarpment, in *Sahyadri: the Great Escarpment of the Indian Subcontinent*, edited by Y. Gunnell and B.P. Radhakrishna, pp. 89-122, Geological Society of India, Bangalore, India.

Gunnell, Y. (2001b) "Fluvial Routing Systems and the Signatures of Onshore Denudation in the Offshore Sedimentary Record of Western India, in *Sahyadri: the Great Escarpment of the Indian Subcontinent*, edited by Y. Gunnell and B.P. Radhakrishna, pp. 279-292, Geological Society of India, Bangalore, India.

Gunnell, Y., and D. Harbor (2008), Structural Underprint and Tectonic Overprint in the Angavo (Madagascar) and Western Ghats (India) — Implications for Understanding Scarp Evolution at Passive Margins, *Journal Geological Society of India*, 71, 763-779.

Gunnell, Y., and L. Fleitout (1998), Shoulder Uplift of the Western Ghats Passive Margin, India: A Denudation Model, *Earth Surface Processes and Landforms*, 23, 391-404, doi: 10.1002/(SICI)1096-9837(199805)23:5<391::AID-ESP853>3.0.CO;2-5.

Harbor, D. and Y. Gunnell (2007), Along-strike escarpment heterogeneity of the Western Ghats: a synthesis of drainage and topography using digital morphometric tools, *Journal Geological Society of India*, 70, 411-426.

Matmon, A., P. Bierman, and Y. Enzel (2002), Pattern and tempo of great escarpment erosion, *Geology*, 30, 1135-1138, doi: 10.1130/0091-7613(2002)030<1135:PATOGE>2.0.CO;2.

Madhavan, Vineeth, (2009), The interplay of climate and landscape evolution along the Western Ghats of India, M.S. Thesis, University of Illinois, Urbana-Champaign, Illinois.

Nesbitt, S. W., and A. M. Anders (2009), Very High Resolution Precipitation Climatologies from the Tropical Rainfall Measuring Mission Precipitation Radar, *Geophysical Research Letters*, 36, L15815, doi: 10.1029/2009GL038026.

Roe, G. H., D. R. Montgomery, and B. Hallet (2002), Effects of Orographic Precipitation Variations on the Concavity of Steady-state River Profiles, *Geology*, 30, 143-46, doi: 10.1130/0091-7613(2002)030<0143:EOOPVO>2.0.CO;2.

Roe, G. H., D. R. Montgomery, and B. Hallet (2003), Orographic Precipitation and the Relief of Mountain Ranges, *Journal of Geophysical Research*, 108, 2315, doi: 10.1029/2001JB001521.

Roe, G.H. (2005), Orographic Precipitation, *Annual Review Earth Planet Science*, 33, 645-671, doi: 10.1146/annurev.earth.33.092203.122541.

Smith, R.B. (1979), The influence of mountains on the atmosphere, *Advances in Geophysics*, 21, 87-230, doi: 10.1016/S0065-2687(08)60262-9.

Strahler, A. N. (1952), Hypsometric (Area-Altitude) Analysis of Erosional Topography, *Bulletin, Geological Society of America*, 63, 1117-142, doi: 10.1130/0016-7606(1952)63[1117:HAAOET]2.0.CO;2

Stock, J.D. and D.R. Montgomery (1999), Geologic constraints on bedrock river incision using the stream power law, *Journal of Geophysical Research*, 104, 4983-4993, doi: 10.1029/98JB02139.

Thomson, S.N., M.T. Brandon, J.H. Tomkin, P.W. Reiners, C. Vasquez, and N.J. Wilson, (2010), Glaciation as a destructive and constructive control on mountain building, *Nature*, 467, 331-317, doi: 10.1038/nature09365.

Tucker, G.E. and R.L. Slingerland, (1994), Erosional dynamics, flexural isostasy, and long-lived escarpments: A numerical modeling study, *Journal of Geophysical Research*, 99, 12,229-12,243, doi: 10.1029/94JB00320.

Turcotte, D. L., and G. Schubert , 2002), Elasticity and Flexure, in *Geodynamics*, 2nd edition, pp. 105-131, Cambridge UP, New York.

Van der Beek, P. and J. Braun (1999), Controls on post-mid-Cretaceous landscape evolution in southeastern highlands of Australia: Insights from numerical surface process models, *Journal of Geophysical Research*, 104, 4945-4966, doi: 10.1029/1998JB900060.

FIGURES AND TABLES

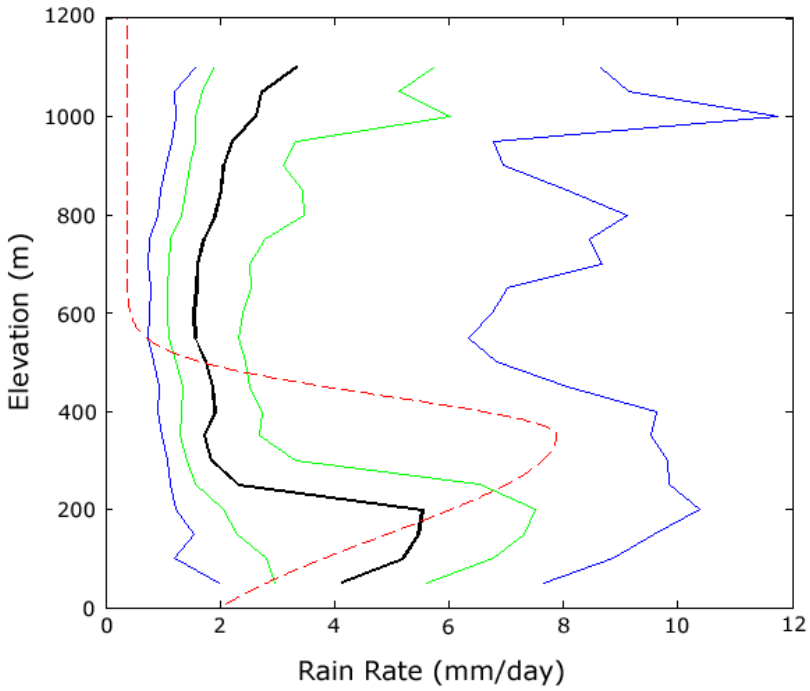

Figure 1. TRMM measurements of precipitation vs. elevation in the Western Ghats of India next to the modeled dynamic rain function. Black line represent average rainfall with two standard deviations to either side in green and blue. The modeled dynamic rain function is shown as a red dashed line.

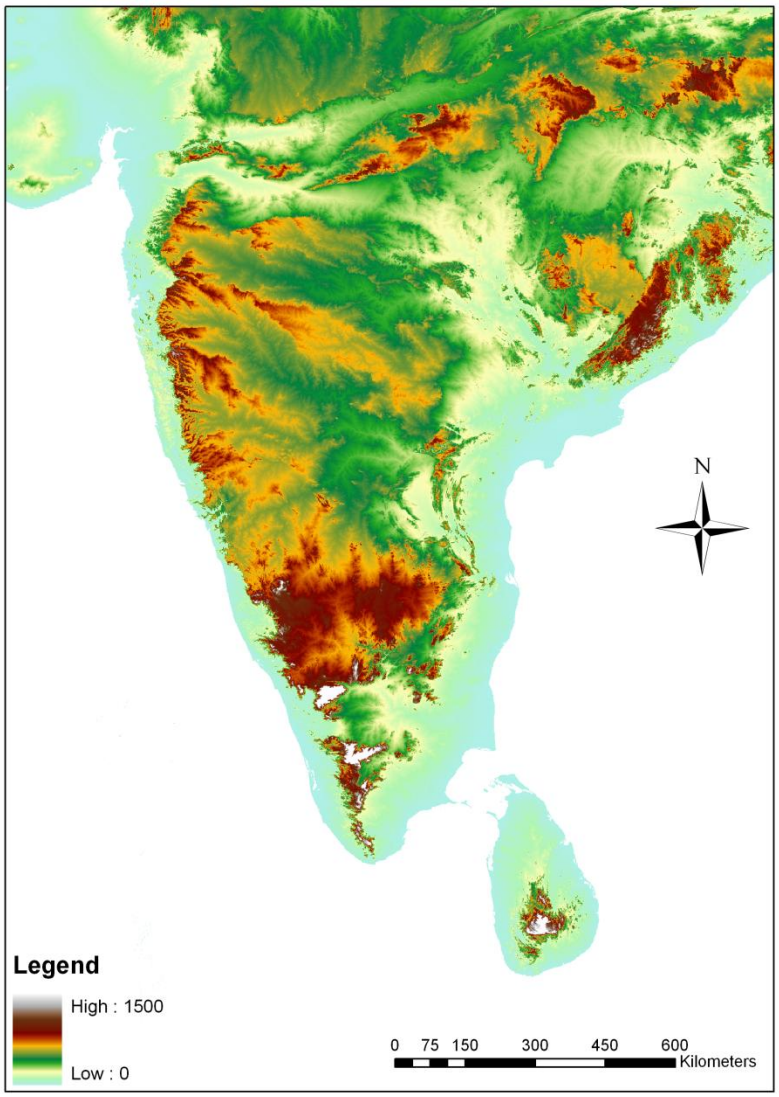

Figure 2. Digital elevation map of the Indian subcontinent. The Western Ghats Great Escarpment is visible running along the western edge of the continent.

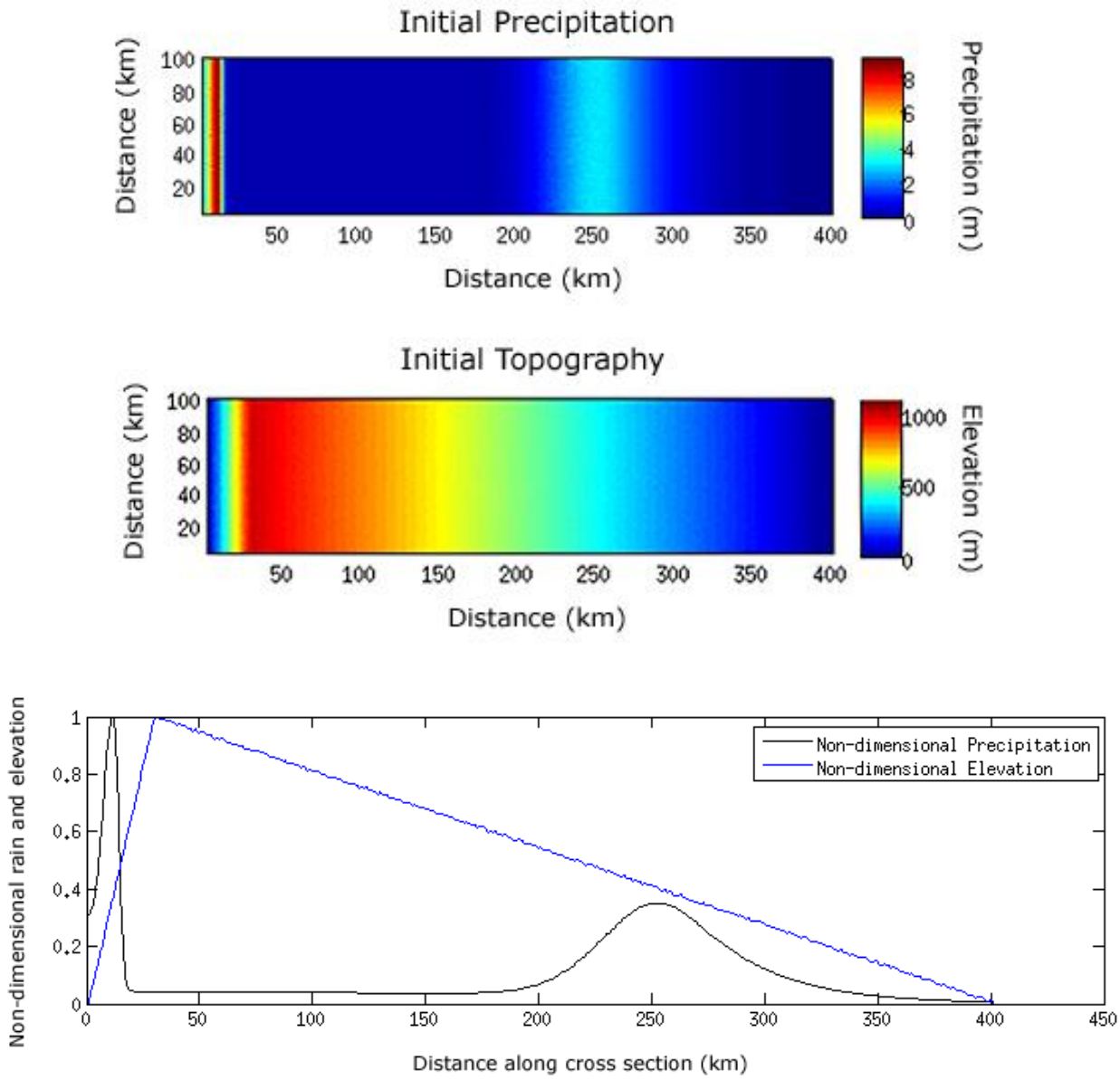

Figure 3. Initial topography and precipitation for run using idealized escarpment in map view and cross section. Cross-section values have been normalized by dividing precipitation (black) and elevation (blue) by their respective maximum values. Dynamic precipitation reaches a maximum at 350 m elevation.

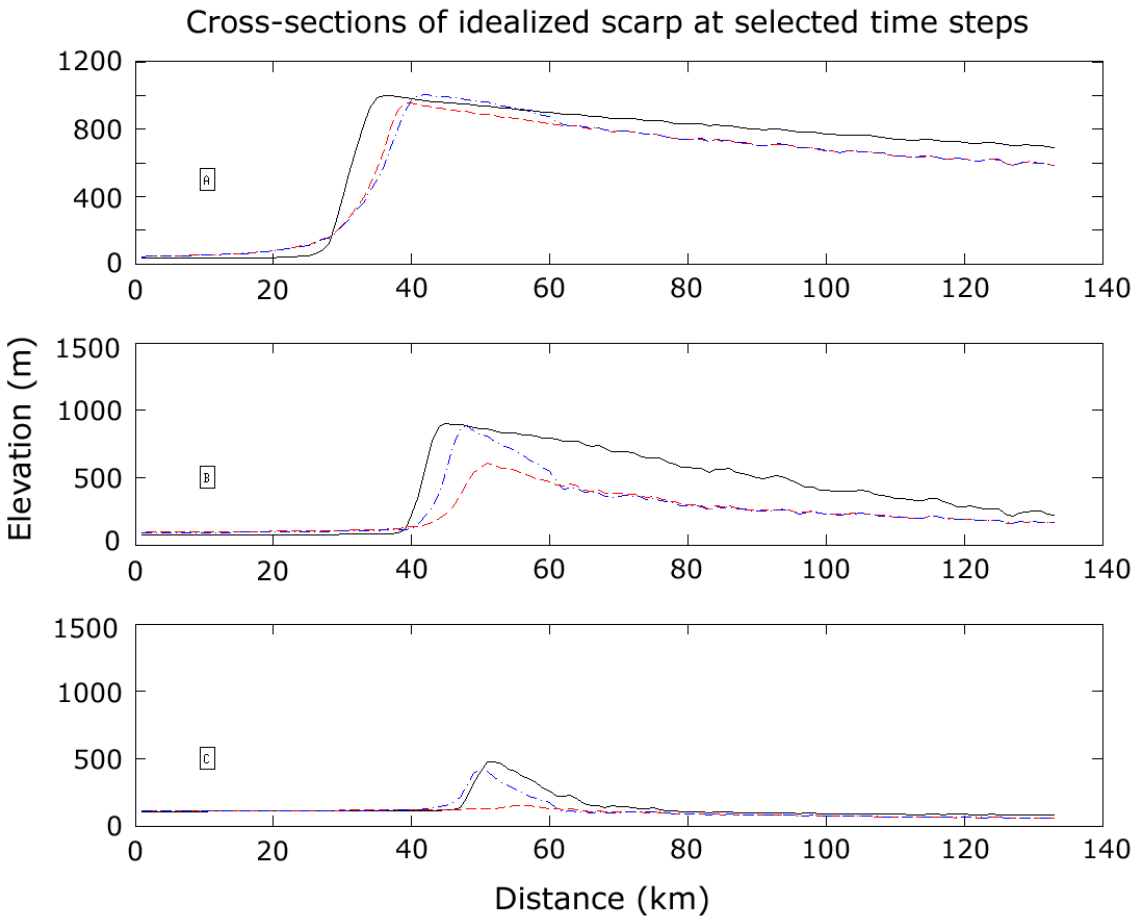

Figure 4. Cross-sections of idealized escarpment for patterned rain, uniform rain, and variable bedrock resistance runs at (a) 12.5 Ma, (b) 25 Ma, and (c) 37.5 Ma. Black solid cross sections show cross sections of patterned rain case. Red dashed cross sections are uniform rain case. Blue dash-dot cross sections have a resistant, crest-parallel bedrock ridge from x=40 to 50 km with bedrock resistance increased by a factor of 2.

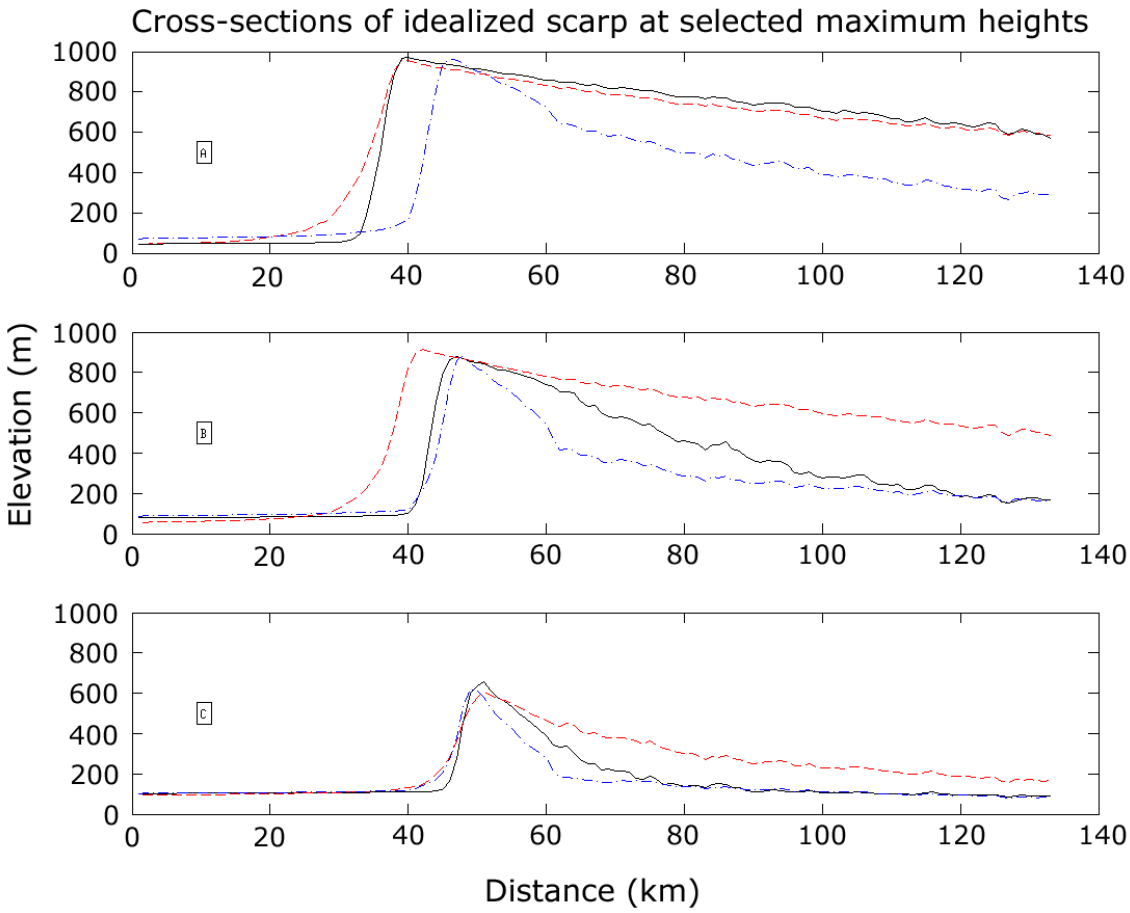

Figure 5. Cross-sections of idealized escarpment for patterned rain, uniform rain, and variable bedrock resistance runs at (a) 95% of initial maximum height, (b) 85% of initial maximum height, and (c) 60% of initial maximum height. Black solid cross sections show cross sections of patterned rain case. Red dashed cross sections are uniform rain case. Blue dash-dot cross sections have a resistant, crest-parallel bedrock ridge from x=40 to 50 km with bedrock resistance increased by a factor of 2.

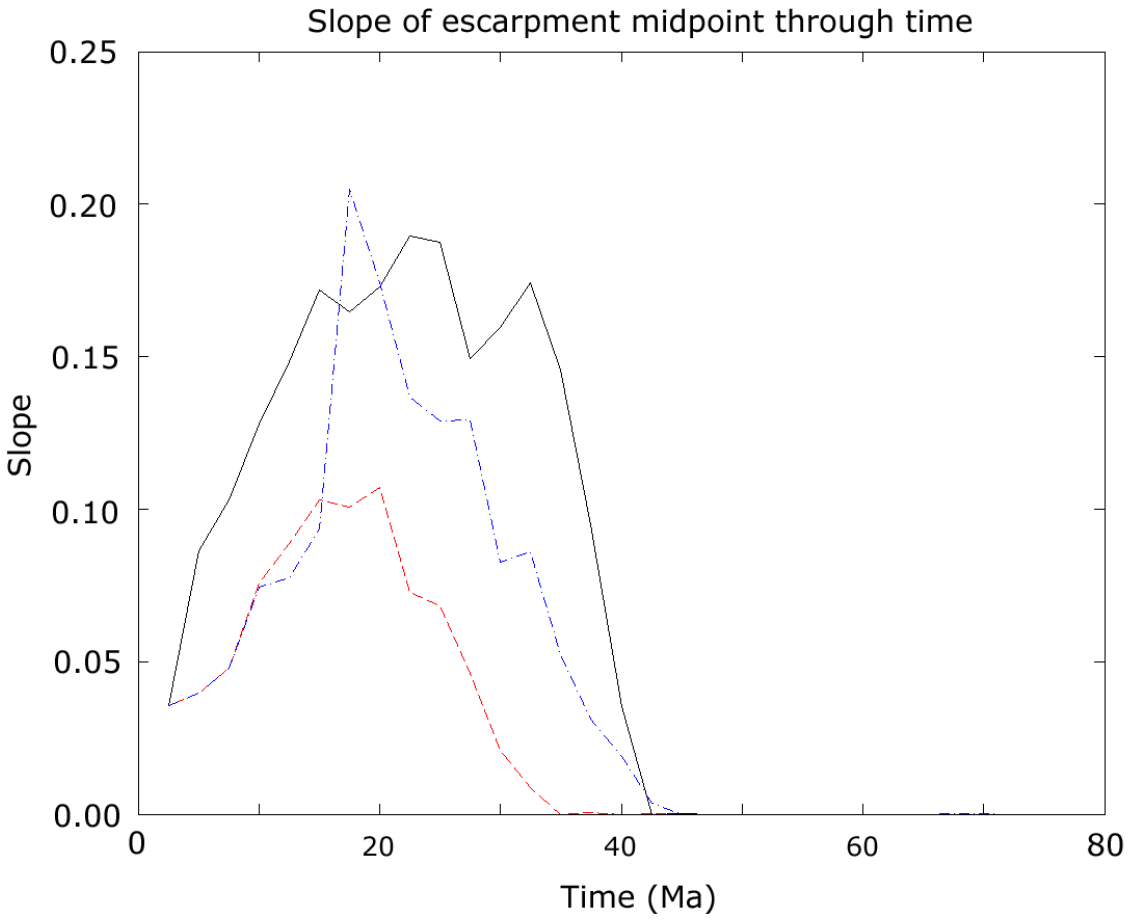

Figure 6. Slope at the mid-point of the escarpment over time for patterned rain (black), uniform rain (red dashed), and bedrock resistance variability (blue dash-dot) runs.

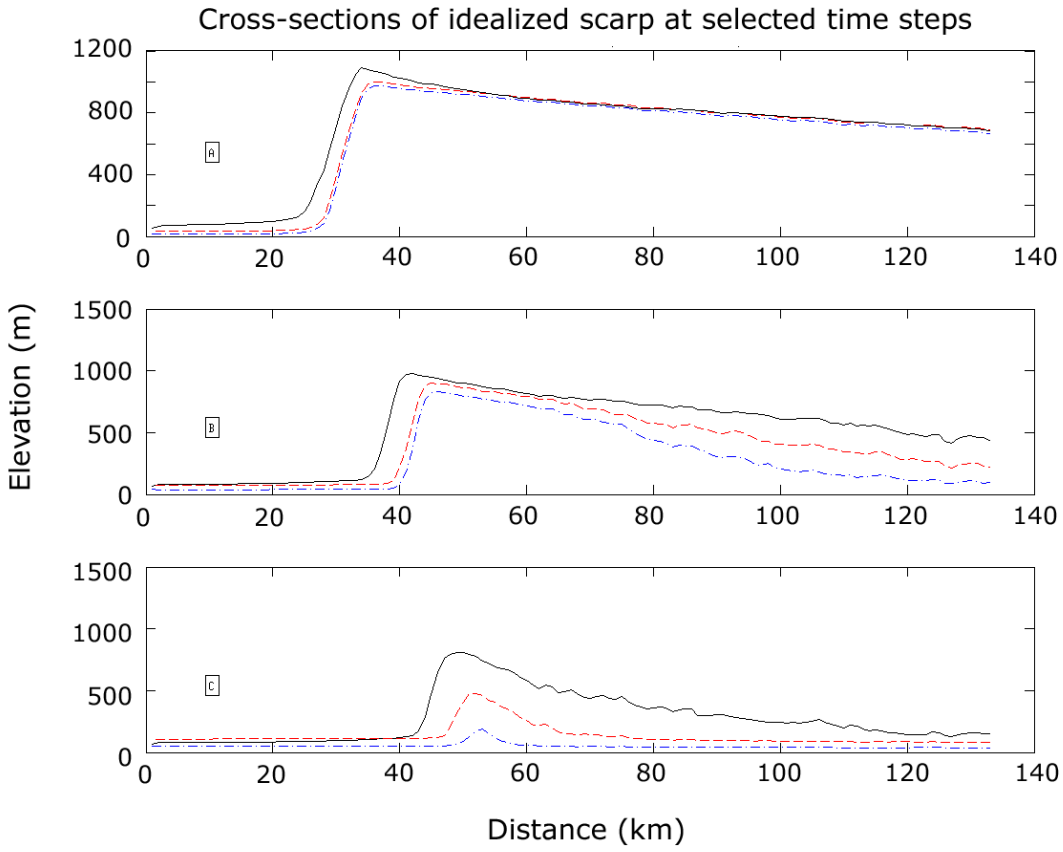

Figure 7. Cross-sections testing flexural sensitivity of idealized escarpment at (a) 12.5 Ma, (b) 25 Ma, and (c) 37.5 Ma. Black solid cross sections have elastic thickness = 5 km. Red dashed cross sections have elastic thickness = 30 km. Blue dash-dot cross sections have elastic thickness = 70 km. Escarpment lifespan increases as elastic thickness decreases.

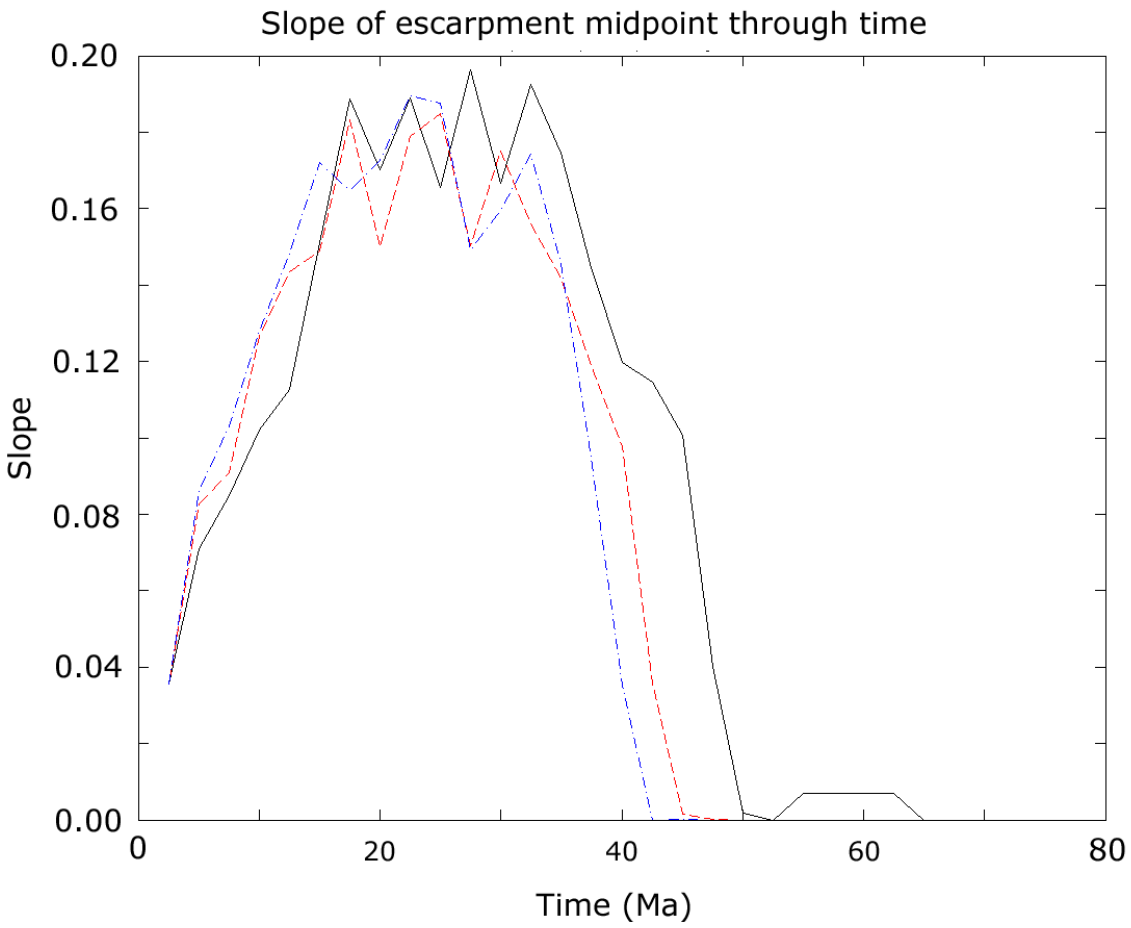

Figure 8. Slope at the mid-point of the escarpment over time for elastic thickness = 5 km (black), 30 km (red dashed), and 70 km (blue dash-dot). Slopes are similar for all cases, though the longer lifespan of the escarpment is visible for lower elastic thicknesses.

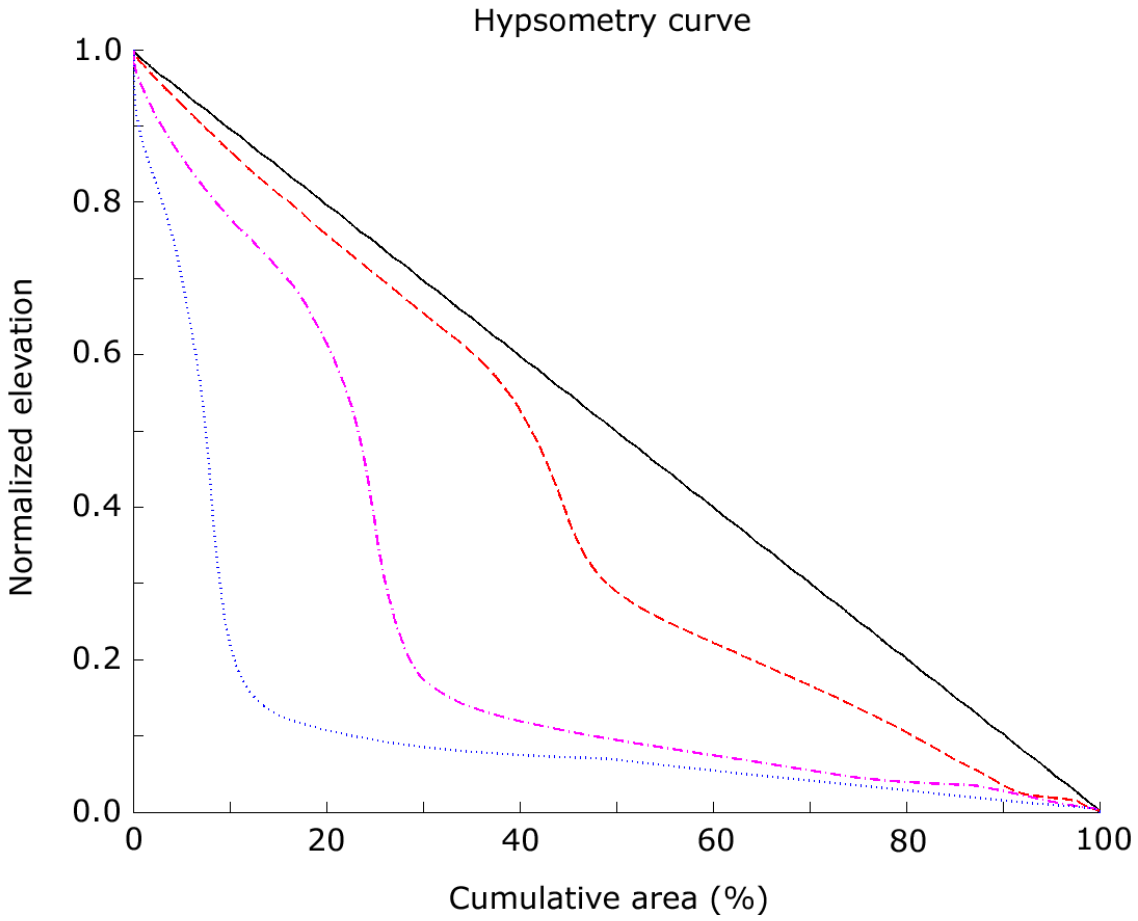

Figure 9. Hypsometric curve for idealized scarp with patterned rain at time=0 Ma (black), 5 Ma (red dashed), 10 Ma (pink dash-dot), 20 Ma (blue dotted).

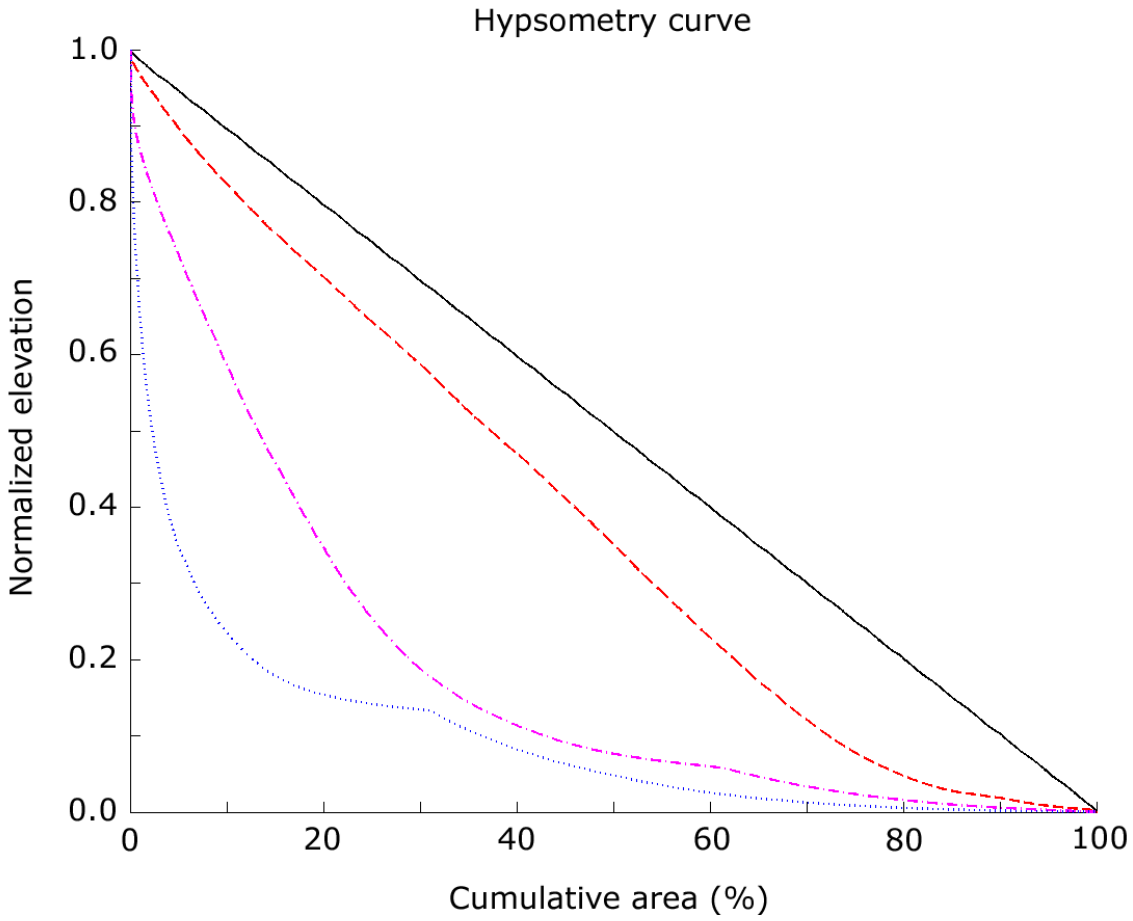

Figure 10. Hypsometric curve for idealized scarp with uniform rain at time=0 Ma (black), 5 Ma (red dashed), 10 Ma (pink dash-dot), 20 Ma (blue dotted).

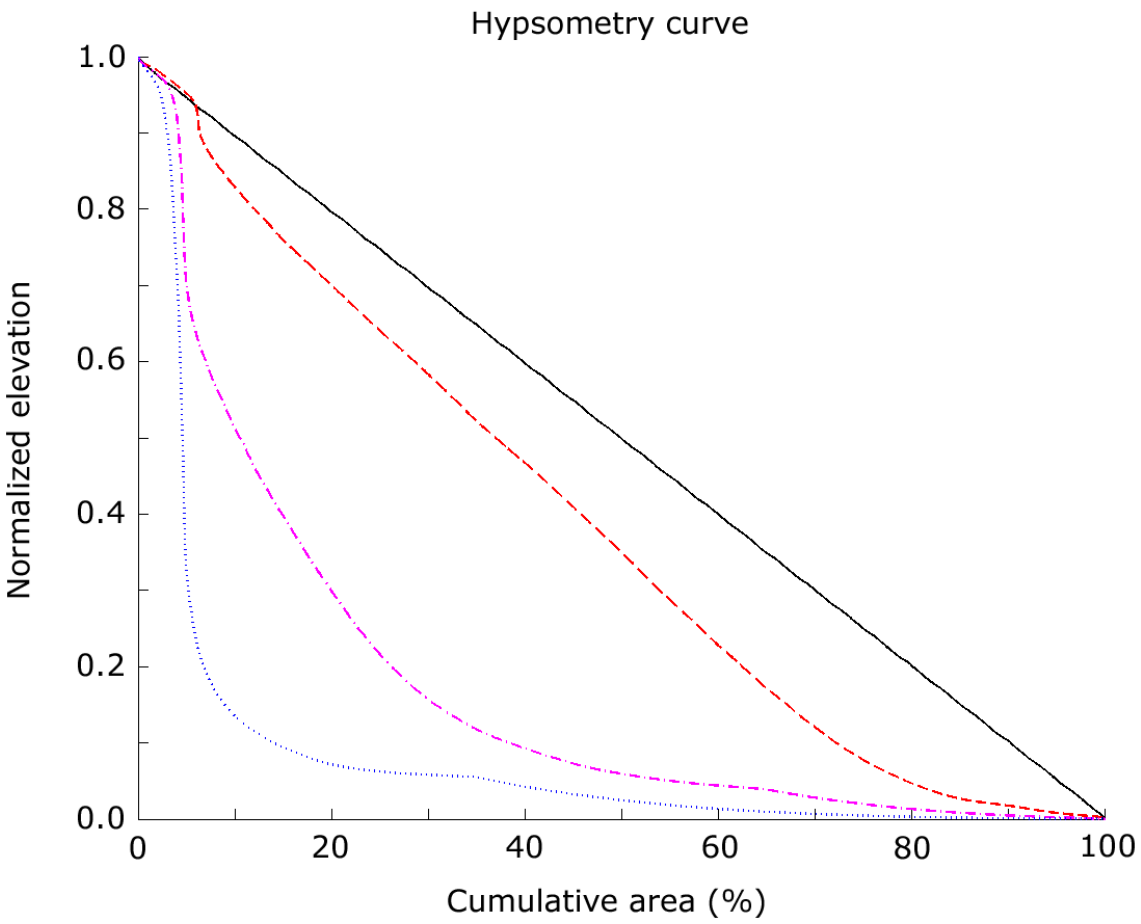

Figure 11. Hypsometric curve for idealized scarp with bedrock with two-times resistance at time=0 Ma (black), 5 Ma (red dashed), 10 Ma (pink dash-dot), 20 Ma (blue dotted).

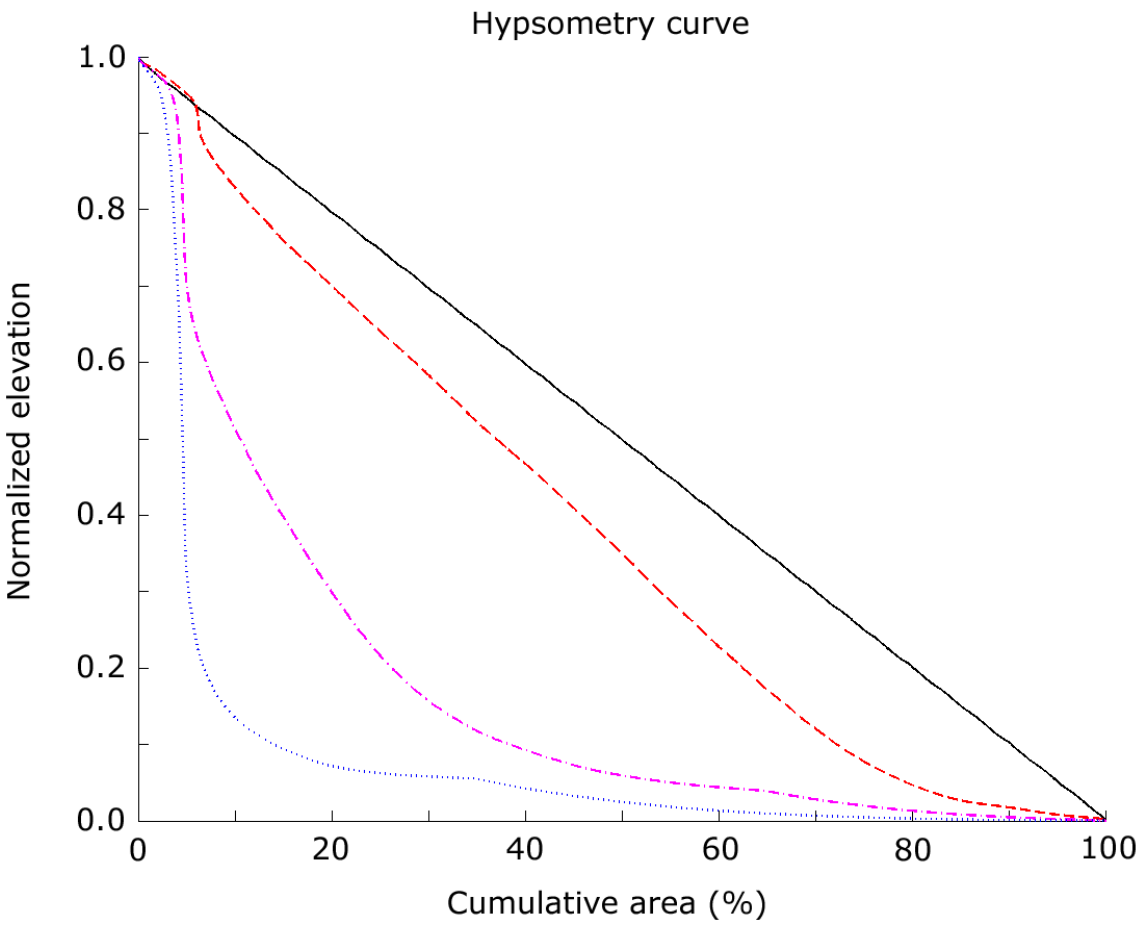

Figure 12. Hypsometric curve for idealized scarp with bedrock with ten-times resistance at time=0 Ma (black), 5 Ma (red dashed), 10 Ma (pink dash-dot), 20 Ma (blue dotted).

Table 1. Run names and variables.

Run name and number		Description	Size (km)	Rain type	Fluvial erosion constant K	Elastic thickness	Time step (yr)	End time (yr)
1	Idealgauss	Idealized scarp	401x101	Dynamic	5.00E-07	30km	500	1.00E+08
2	Idealuni	Idealized scarp	401x101	Uniform (0.7935 m/yr)	5.00E-07	30km	500	1.00E+08
3	IdealuniBR	Idealized scarp with resistant ridge from x = 40-50 km, k= 2.50e-07	401x101	Dynamic	5.00E-07	30km	500	1.00E+08
4	IdealuniBR2	Idealized scarp with resistant ridge from x = 40-50 km, k= 5.00e-08	401x101	Uniform (0.7935 m/yr)	5.00E-07	30km	500	1.00E+08
5	IdealFlex1	Idealized sensitivity test of elastic thickness (h elastic)	401x101	Dynamic	5.00E-07	5km	500	1.00E+08
6	IdealFlex2	Idealized sensitivity test of h elastic	401x101	Dynamic	5.00E-07	15km	500	1.00E+08
7	IdealFlex3	Idealized sensitivity test of h elastic	401x101	Dynamic	5.00E-07	50km	500	1.00E+08
8	IdealFlex4	Idealized sensitivity test of h elastic	401x101	Dynamic	5.00E-07	70km	500	1.00E+08

Table 2. Lifespan of the escarpment for different model runs.

Run name	Elastic thickness of the lithosphere (km)	Precipitation function	Bedrock resistance	Escarpment lifespan (Ma)
IdealFlex1	5	Patterned	Uniform	44 Ma
IdealGauss	30	Patterned	Uniform	37 Ma
Ideal Flex4	70	Patterned	Uniform	34 Ma
IdealUni	30	Uniform	Uniform	25 Ma
IdealBR2	30	Uniform	Resistant ridge	35 Ma
IdealBR10	30	Uniform	Resistant ridge	100+ Ma